

# Chapter 3

## Effect of transport on composition.

### Supplemental Reading:

Holton (1979), pp. 40–4

Houghton (1977), pp. 81–2, 55–8

### 3.1 General considerations

In this chapter, we once again turn to a simple model. However, here we will be closer to an approximation than we were in the previous chapter. The model here will provide greater scope to engage in simulating observations. It also provides an example of how a model can, indeed, offer insights into the physics.

Consider a chemical constituent,  $i$ , with density  $\rho_i(z, \theta)$  and a photochemical equilibrium distribution  $\bar{\rho}_i(z, \theta)$ . Let us consider an idealized situation where, in the absence of transport,

$$\frac{\partial \rho_i}{\partial t} = \alpha(z, \theta)(\bar{\rho}_i(z, \theta) - \rho_i(z, \theta)), \quad (3.1)$$

where  $z$  is altitude and  $\theta$  is latitude. Equation 3.1 may be considered as a highly idealized description of ozone.

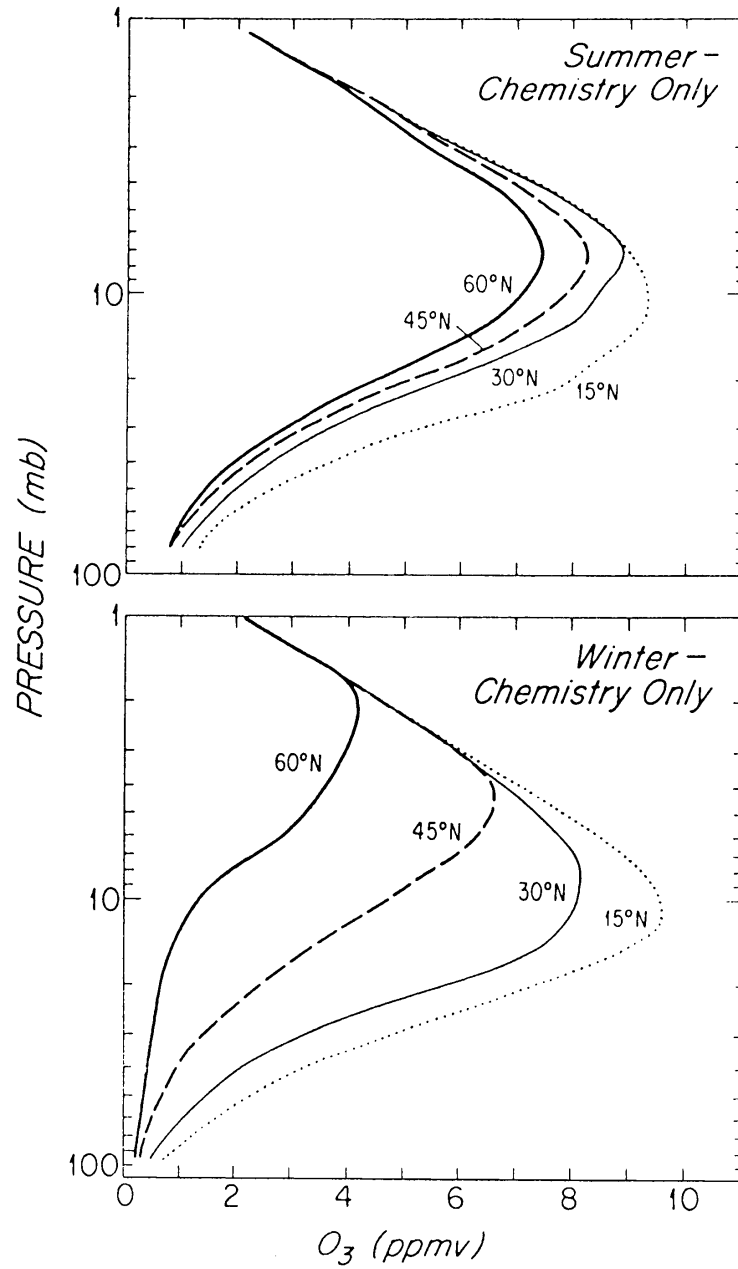


Figure 3.1: Photochemical equilibrium distributions of ozone mixing ratio with pressure at various latitudes for winter and summer. Note that this and the following three figures were prepared by S. Wofsy in 1980. They are not state of the art calculations; this doesn't particularly matter for the crude arguments of this chapter.

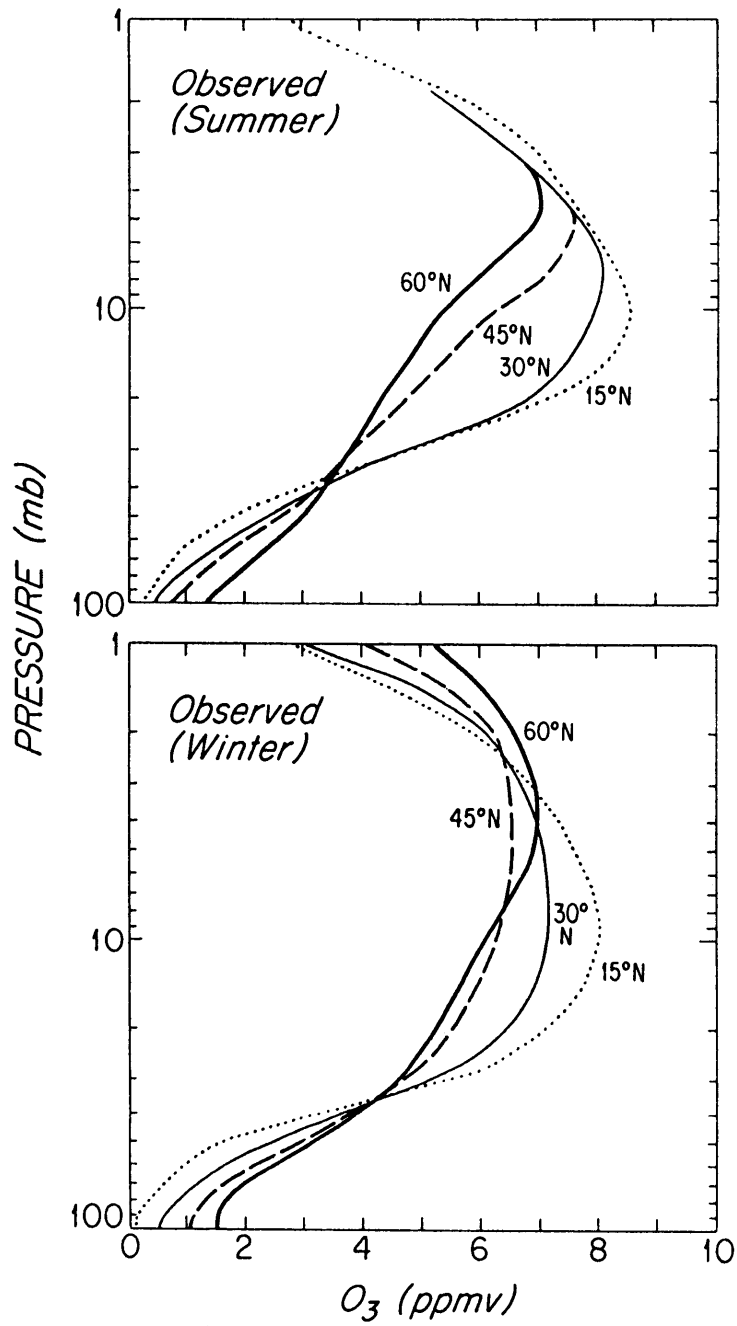


Figure 3.2: Observed distributions of ozone mixing ratio with pressure at various latitudes for winter and summer.

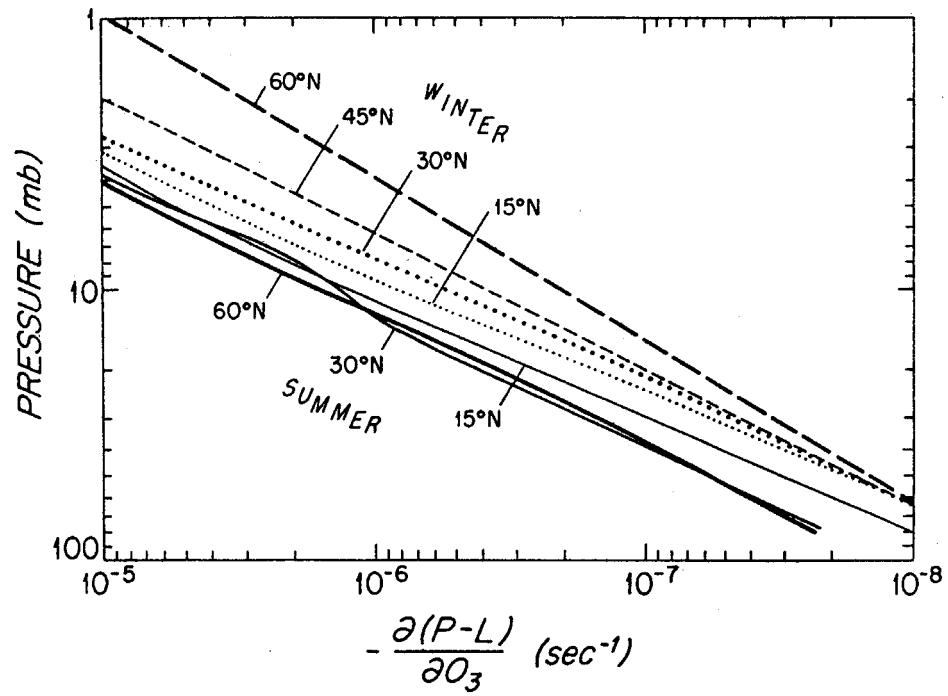


Figure 3.3: Photochemical relaxation rate for ozone as a function of pressure for various latitudes. This rate is estimated by differentiating the difference between ozone loss and production with respect to changes in ozone.

Figure 3.1 shows the distribution of  $\bar{p}_i(z, \theta)$  (for ozone); Figure 3.2 shows the observed distribution; Figure 3.3 shows the photochemical relaxation time ( $\alpha^{-1}$ ). A comparison of Figures 3.1 and 3.2 shows that atmospheric ozone is, in most regions, not in photochemical equilibrium. A notable exception is the tropical upper stratosphere. The differences between the observed and photochemical equilibrium distributions become particularly clear when we focus on column densities (i.e., the total ozone per unit area above a given point).

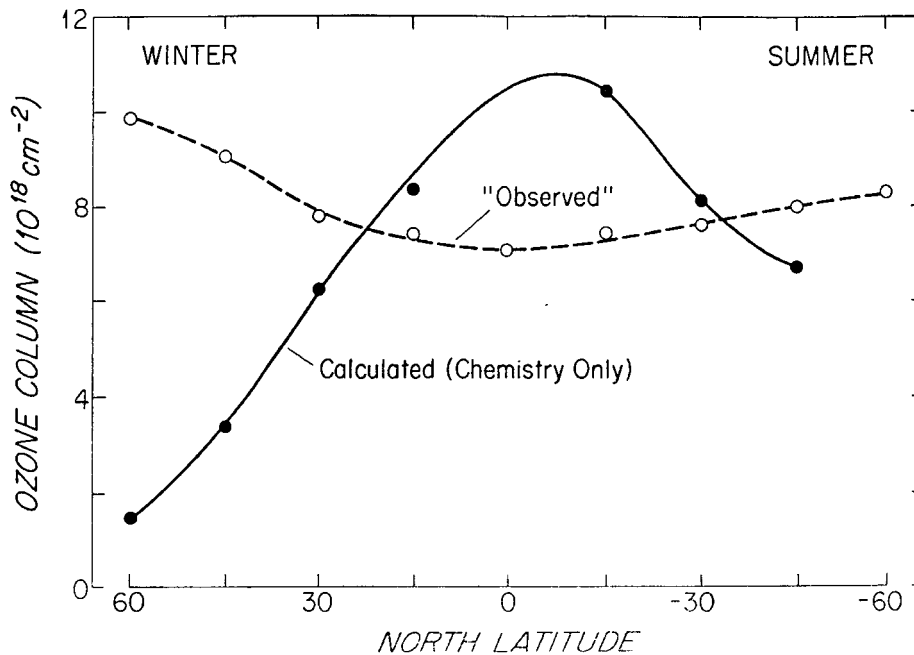


Figure 3.4: Observed and calculated (on the basis of photochemical equilibrium) distributions of ozone column density with latitude in the northern hemisphere for both winter and summer.

These are shown in Figure 3.4. We see that the equilibrium distribution has a maximum over the equator, and decreases toward the poles in both summer and winter – with the winter minimum being much deeper. The observed distribution has a minimum at the equator and rises toward the poles, with the winter maximum being greater than the summer maximum.

### 3.1.1 Equations of continuity

We wish, now, to examine the rôle of a large-scale motion field in causing  $\rho_i$  to differ from  $\bar{\rho}_i$ . To do this we must introduce the equation of mass continuity.

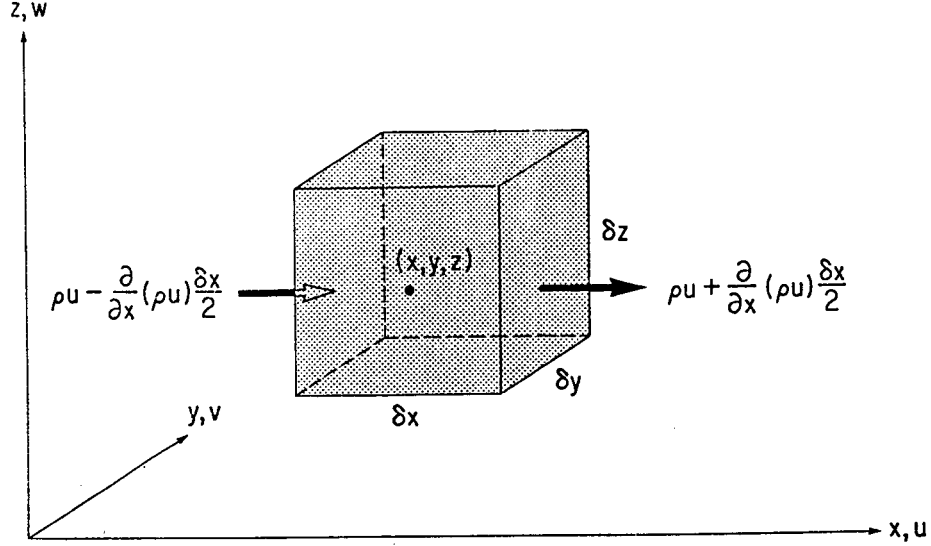


Figure 3.5: Schematic depiction of mass flow and continuity.

Consider a fixed element of volume in cartesian coordinates (*viz.* Figure 3.5):

$$\begin{aligned} \frac{\partial \rho}{\partial t} \delta x \delta y \delta z &= \\ & \left[ \rho u - \frac{\partial}{\partial x}(\rho u) \frac{\delta x}{2} \right] \delta y \delta z - \left[ \rho u + \frac{\partial}{\partial x}(\rho u) \frac{\delta x}{2} \right] \delta y \delta z \\ & + \left[ \rho v - \frac{\partial}{\partial y}(\rho v) \frac{\delta y}{2} \right] \delta x \delta z - \left[ \rho v + \frac{\partial}{\partial y}(\rho v) \frac{\delta y}{2} \right] \delta x \delta z \\ & + \left[ \rho w - \frac{\partial}{\partial z}(\rho w) \frac{\delta z}{2} \right] \delta x \delta y - \left[ \rho w + \frac{\partial}{\partial z}(\rho w) \frac{\delta z}{2} \right] \delta x \delta y. \end{aligned}$$

As  $\delta x, \delta y, \delta z \rightarrow 0$ , we get

$$\frac{\partial \rho}{\partial t} = -\nabla \cdot (\rho \vec{u}). \quad (3.2)$$

In a similar manner (3.1) may be generalized to

$$\frac{\partial \rho_i}{\partial t} + \nabla \cdot (\rho_i \vec{u}) = \alpha(\bar{\rho}_i - \rho_i). \quad (3.3)$$

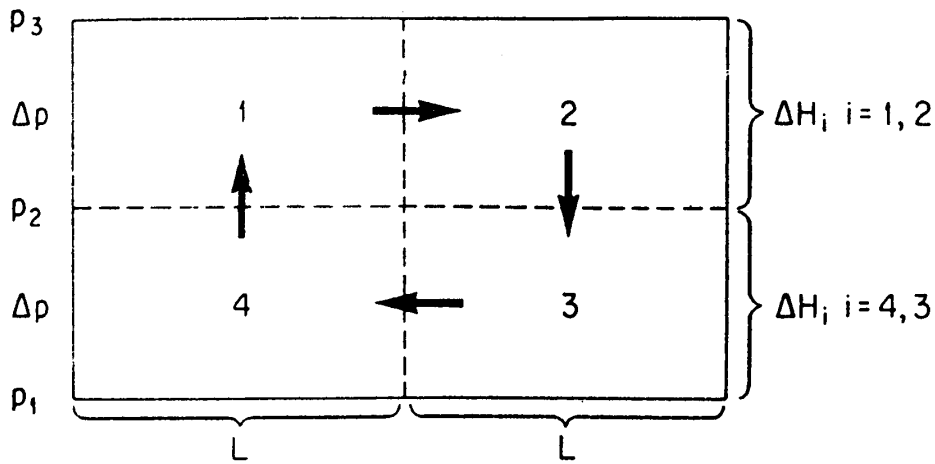


Figure 3.6: 4-box geometry for studying effect of transport on a chemically active constituent.

### 3.2 4-box transport model

We next wish to apply (3.2) and (3.3) to a very simplified geometry where  $\vec{u}$  is specified (*viz.* Figure 3.6). Each of the four boxes has the same basic mass (i.e.,  $p_2 = p_1 - \Delta p$ ;  $p_3 = p_2 - \Delta p$ ). At each interface we will assume the velocity to have a characteristic magnitude  $V$  (at vertical surfaces) or  $W$  (at horizontal surfaces). Finally, we assume that each box can be characterized by single values of  $\alpha_j$ ,  $(\rho_i)_j$ ,  $(\bar{\rho}_i)_j$ , and  $\rho_j$ , where  $j = \text{box number}$  (Note,  $\rho_j$  refers to the mean density of air in the  $j^{\text{th}}$  box,  $(\rho_i)_j$  to the density of the  $i^{\text{th}}$  constituent in the  $j^{\text{th}}$  box, and  $(\bar{\rho}_i)_j$  to the photochemical equilibrium density of the  $i^{\text{th}}$  component in the  $j^{\text{th}}$  box.). This approach is, of course, extremely crude, but it is adequate for illustrative purposes.

Let us first integrate Equation 3.2 over box 1 (we are assuming a steady state where  $\frac{\partial}{\partial t} = 0$ ):

$$\begin{aligned} \int_{\text{box 1}} \nabla \cdot \rho \vec{u} \, dy \, dz &= \int_{\text{perimeter of box 1}} \rho u_n \, dl \\ &= \rho_1 V \Delta H_1 - \rho_4 W L = 0. \end{aligned}$$

This implies

$$\rho_1 V \Delta H_1 = \rho_4 W L = M. \quad (3.4)$$

Making use of hydrostaticity<sup>1</sup>,

$$\Delta H_1 \cong \frac{\Delta P}{\rho_1 g}$$

so (3.4) becomes

$$\frac{\Delta P}{g} V = \rho_4 W L = M. \quad (3.5)$$

More generally, the mass flux across each interface must equal  $M$ . (As a practical matter,  $W$  may have to be considered different according to whether it is going up or down.)

Integrating Equation 3.3 over box 1 we get

$$(\rho_i)_1 V \Delta H_1 - (\rho_i)_4 W L = \alpha_1 ((\bar{\rho}_i)_1 - (\rho_i)_1) L \Delta H_1 \quad (3.6)$$

and, using (3.5),

$$\frac{(\rho_i)_1}{\rho_1} M - \frac{(\rho_i)_4}{\rho_4} M = \alpha_1 \frac{\Delta P}{g} L \left( \frac{(\bar{\rho}_i)_1}{\rho_1} - \frac{(\rho_i)_1}{\rho_1} \right)$$

or, more generally,

$$\left( \frac{\rho_i}{\rho} \right)_j M - \left( \frac{\rho_i}{\rho} \right)_{j-1} M = \alpha_j \frac{\Delta P}{g} L \left( \left( \frac{\bar{\rho}_i}{\rho} \right)_j - \left( \frac{\rho_i}{\rho} \right)_j \right)$$

---

<sup>1</sup>If the reader doesn't know what this is, it is discussed in Chapter 4.



or, equivalently,

$$R \left[ \left( \frac{\rho_i}{\rho} \right)_j - \left( \frac{\rho_i}{\rho} \right)_{j-1} \right] = \alpha_j \left( \left( \frac{\bar{\rho}_i}{\rho} \right)_j - \left( \frac{\rho_i}{\rho} \right)_j \right) \quad (3.7)$$

where

$$R = \frac{Mg}{\Delta P L} = \frac{V}{L}$$

and

$$\begin{aligned} j &= 1, 2, 3, 4 \\ j-1 &= 4, 1, 2, 3 \end{aligned}$$

(i.e.,  $j$  is a cyclic index where  $j = j + 4$ ).

Several important points are to be noted concerning (3.7):

1. The dimension of both  $R$  and  $\alpha_j$  is  $1/[T]$  (i.e., 1/time).
2. The left-hand side of (3.7) represents the rate at which advection is acting to eliminate differences in  $(\frac{\rho_i}{\rho})$  between adjacent boxes. Note that advection acts to homogenize the mixing ratio of constituent  $i$ ,  $(\frac{\rho_i}{\rho})$ , rather than its density,  $\rho_i^2$ .

---

<sup>2</sup>A somewhat more elegant approach to this feature can be obtained directly from Equations 3.2 and 3.3. Rewrite

$$\rho_i = \frac{\rho_i}{\rho} \rho.$$

Then

$$\begin{aligned} \frac{\partial \rho_i}{\partial t} + \nabla \cdot (\rho_i \vec{u}) &= \rho \frac{\partial}{\partial t} \left( \frac{\rho_i}{\rho} \right) + \frac{\rho_i}{\rho} \frac{\partial \rho}{\partial t} \\ &+ \rho \vec{u} \cdot \nabla \left( \frac{\rho_i}{\rho} \right) + \frac{\rho_i}{\rho} \nabla \cdot (\rho \vec{u}) \end{aligned}$$

3. The right-hand side of (3.7) represents the rate at which chemistry is acting to bring  $(\frac{\rho_i}{\rho})$  to its equilibrium value,  $(\frac{\bar{\rho}_i}{\rho})$ .
4. The non-dimensional parameter  $R/\alpha$  represents the balance in the competition between the two processes described in items (2) and (3). When  $R/\alpha \gg 1$ , there is a tendency for  $(\frac{\rho_i}{\rho})_j$  to approach  $(\frac{\bar{\rho}_i}{\rho})_{j-1}$ , whereas when  $R/\alpha \ll 1$ , there is a tendency for  $(\frac{\rho_i}{\rho})_j$  to approach its chemical equilibrium value.

Our object is to solve (3.7) for  $(\frac{\rho_i}{\rho})_j$ . This is facilitated by rewriting (3.7) as

$$(R + \alpha_j)\phi_j - \alpha_j\bar{\phi}_j = R\phi_{j-1}, \quad (3.8)$$

where

$$\phi_j \equiv \left(\frac{\rho_i}{\rho}\right)_j.$$

Successive substitution in (3.8) yields

$$\begin{aligned} \phi_j \left(1 - \frac{R^4}{R_{1,2,3,4}}\right) = & \frac{\alpha_j\bar{\phi}_j}{R_j} + \frac{R\alpha_{j-1}\bar{\phi}_{j-1}}{R_{j,j-1}} \\ & + \frac{R^2\alpha_{j-2}\bar{\phi}_{j-2}}{R_{j,j-1,j-2}} + \frac{R^3\alpha_{j-3}\bar{\phi}_{j-3}}{R_{1,2,3,4}}, \end{aligned} \quad (3.9)$$

where

---


$$= \rho \left\{ \frac{\partial}{\partial t} \left(\frac{\rho_i}{\rho}\right) + \vec{u} \cdot \nabla \left(\frac{\rho_i}{\rho}\right) \right\} = \alpha(\bar{\rho}_i - \rho_i)$$

and

$$\frac{\partial}{\partial t} \left(\frac{\rho_i}{\rho}\right) + \vec{u} \cdot \nabla \left(\frac{\rho_i}{\rho}\right) = \alpha \left(\frac{\bar{\rho}_i}{\rho} - \frac{\rho_i}{\rho}\right).$$

$$\begin{aligned}
R &\equiv \frac{V}{L} \\
R_j &\equiv (R + \alpha_j) \\
R_{j,k} &\equiv (R + \alpha_j)(R + \alpha_k) \\
R_{j,k,l} &\equiv (R + \alpha_j)(R + \alpha_k)(R + \alpha_l) \\
R_{1,2,3,4} &\equiv (R + \alpha_1)(R + \alpha_2)(R + \alpha_3)(R + \alpha_4).
\end{aligned}$$

The reader should attempt to interpret (3.9). For example,  $\phi_j$  clearly depends on the value of  $\bar{\phi}$  in each of the boxes, weighted by measures of transport efficiency.

A particularly interesting solution exists in the following limit:

$$\begin{aligned}
\alpha_1 &\gg R \\
\alpha_2, \alpha_3, \alpha_4 &\ll R.
\end{aligned}$$

Then

$$\begin{aligned}
R_1 &\approx +\alpha_1 \\
R_j &\approx R \text{ for } j \neq 1
\end{aligned}$$

and from (3.9)

$$\begin{aligned}
\phi_1 &\approx \overline{\phi_1} \\
\phi_2 &\approx \overline{\phi_1} \\
\phi_3 &\approx \overline{\phi_1} \\
\phi_4 &\approx \overline{\phi_1}
\end{aligned}$$

Note, that in this limit, the answer does *not* depend on the sign of  $M$  (or  $V$ ). Also, in the event that  $\overline{\phi_1} \gg \overline{\phi_2}, \overline{\phi_3}$ , the column density of ‘ozone’ below boxes 2 and 3 has been greatly increased by transport (beyond what would be implied by photochemical equilibrium). (What would one have to do to make the column density below boxes 2 and 3 greater than it is below boxes 1 and 4? How might this relate to Figure 3.4?)